Formation of a glassy solid by computer simulation

Kazumasa Shinjo
Nippon Telegraph and Telephone Corporation, Basic Research Laboratories, Musashino, Tokyo 180, Japan
(Received 27 March 1989; revised manuscript received 12 June 1989)

The Hamiltonian dynamics of a Lennard-Jones system is examined to study the formation process of a glassy solid, by using the mapping-onto-minima method. Four types of dynamics are found, which depend on temperature regimes classified by three characteristic temperatures T_1, T_2, and T_3. (1) The high-temperature regime $T_1 \leq T$: The state point describing the system of motion wanders over various local minima. (2) The intermediate-temperature regime $T_2 \leq T < T_1$: The state point wanders over an energetically widely spread local minimum for a specific time interval after the system cooling stops but gradually tends to stay in the single local minimum or a few local minima. (3) The low–intermediate-temperature regime $T_3 \leq T < T_2$: The state point assumes the several local minima intermittently and finally relaxes into a single local minimum or a few local minima with almost equal potential energies. The crystallization occurs stepwise by wandering over several local minima. (4) The low-temperature regime $T < T_3$: The state point stays in the single local minimum or a few local minima with almost equal potential energy for the entire time interval. From the observation that the number of the local minima over which the state point wanders decreases drastically for $T < T_2$, it is concluded that T_2 corresponds to the glass transition temperature, and a glassy solid is formed for $T < T_2$. The distances between the local minima over which the state point wanders are also studied for each temperature regime. It is found that the small (or large) distances between the local minima generally correspond to the small (or large) differences of the potential energies at the local minima. The stepwise-occurring crystallization is discussed by examining the diffusion length of each particle, and it is found that the crystallization appears as a result of a cascade diffusion of particles, triggered by a few particles.

I. INTRODUCTION

If a liquid is cooled quickly enough to below freezing, it enters a supercooled-liquid state, bypassing crystallization. If cooled further, the supercooled liquid begins to solidify, and a liquid-solid transition generally occurs. This phenomenon is often called "glass transition."[1,2] A glass transition is a morphological transition of a system from a liquid to a noncrystalline solid. Here a noncrystalline solid means the supercooled liquid which has a relaxation time so long it can be considered a solid rather than a liquid.

Many attempts have been made[3–13] to learn about glass transition, as well as the structural and dynamic properties of glass, by use of molecular dynamics and Monte Carlo techniques. The question of how a computer simulates the properties of the glass-forming liquids has been studied.

The formation of a glassy solid at very low temperature and the existence of the glass transition have been concluded from the following: A glassy solid formation was ascribed to the observations that at very low temperatures the particles do not diffuse over a typical simulation time scale,[6] the second peak of the radial distribution function is split into two subpeaks as temperature decreases like that of metallic glasses[9,11] and others. The existence of the glass transition was based on the following observation:[12] The existence of the transition most likely resulted from the fact that density and enthalpy are approximately linear functions of temperature at both low and high temperatures. This approximate linearity ensures that thermal expansion coefficients and heat capacity, being constant at both low and high temperatures, indicate that there is a region in between, which is called the transition region. Next, by examining the behavior of the physical properties around the transition temperature, it was concluded that the transition is qualitatively analogous to glass transition.

However, the above conclusions are questionable because of the following reasons: No appreciable diffusion in simulation is dependent on the observation time length and there is no reasonable criterion for concluding no diffusion of particle. Further, it was shown[13] that the linearity described above depends strongly on the cooling procedure. Stepwise cooling results in approximate linearity of the density versus temperature curve at both low and high temperatures, but continuous cooling does not. With continuous cooling, the density curve is mild over the entire temperature region, so the thermal expansion coefficient changes over the entire temperature region. Discussions of whether the simulated glass is similar to that produced in a laboratory or not, generally depend on which experimental data are chosen.

A picture of a glassy solid has been proposed[14] in connection with the shape of the multidimensional potential surface of all particles. This picture bypasses discussing the direct comparison of physical quantities, which makes the glassy solid picture clearer. The mechanical

and thermodynamic properties of a glassy solid are derived from the formation of the local minima or the potential barriers. The potential barriers prevent the state point of the system from escaping the local minima. The smaller the total kinetic energy, the smaller the probability of the state point escaping from the local minimum. Relaxation time for the structure tends to infinity as total kinetic energy or temperature decreases. According to this picture, the direct proof of the formation of the glassy solid at a very low temperature is to see whether the local minima or the potential barriers are formed on the potential surface during system cooling. Here, the local minima should have a configuration with amorphous packing of particles. The formation of local minima has already been confirmed for the Lennard-Jones (LJ) type system.[15,16] Thus, the LJ system is the glass-forming system even though it has never formed glass under laboratory conditions.[17]

To study the formation process of a glassy solid, we examine the Hamiltonian dynamics after the system is cooled to various temperatures. A formation process of a glassy solid will be discussed in connection with the temperature dependence of dynamics.

II. MODEL AND METHOD

A. Model

Let us consider a system consisting of many classical particles in which the total energy is decomposed into total kinetic energy plus total potential energy. Total kinetic energy and total potential energy are defined, respectively, by the sum of the kinetic energies for each particle, and by one-half the sum of the interaction potential between particles. For the thermodynamic limit, the total kinetic energy, denoted by $E_k[p_i^\alpha(t)]$ is related via the virial theorem to the temperature $T[p_i^\alpha(t)]$:

$$T[p_i^\alpha(t)]=\sum_{i,\alpha} p_i^\alpha(t)^2/3Nm\,(=2E_k[p_i^\alpha(t)]/3)$$

(N is the total number of particles and m is the mass of one particle). The suffix i specifies the particle and α stands for the direction of real space x, y or z. The $p_i^\alpha(t)$ is the α component of the momentum of the ith particle at time t. Notations such as $T[p_i^\alpha(t)]$ and $E_k[p_i^\alpha(t)]$ are introduced to show that these quantities depend on many variables such as a set of $r_i^\alpha(t)$ and $p_i^\alpha(t)$. In the following, similar notations are used. Total potential energy, denoted by $V[r_i^\alpha(t)]$, is a function of the position coordinates of all particles, where $r_i^\alpha(t)$ stands for the α component of the position coordinate of the ith particle at time T. The total potential energy spans a $3N$-dimensional space, called a potential-energy surface or simply a potential surface. It is simply expressed in terms of the notation of total potential energy. The state point describing the system of motion moves on the potential surface $V[r_i^\alpha(t)]$ whose kinetic energy is $E_k[p_i^\alpha(t)]$. In the following, the often-studied system of 108 Lennard-Jones particles is assumed. Mutual interaction is described by the LJ-type interaction potential

$$v(r)=\varepsilon[(\delta/r)^{12}-(\delta/r)^6]\ ,$$

where r is the interdistance between particles. Parameters are chosen for the argon particles: $\varepsilon=167\times10^{-16}$ erg, $\delta=3.40$ Å, and $m=6.69\times10^{-26}$ kg.

B. Method

The $p_i^\alpha(t)$ and $r_i^\alpha(t)$ are traced by solving the Newtonian equation of motion of particles.[11,18] The equation is integrated at each time step Δt, where Δt is 2×10^{-14} sec. A periodic boundary condition is imposed, which has a periodicity specified by length $L(t)$. Length $L(t)$ is adjusted to maintain atmospheric pressure. Cooling is performed by scaling the momentum for each particles. The cooling ratio is taken to be 1.25×10^{12} K/sec.

The motion of the state point is traced by using the mapping-onto-minima method explored by Stillinger and Weber.[16] This method is superior to others since the dynamics of the state point in the $3N$-dimensional space is represented by a set of local minima with a countable measure. A set of position coordinates $r_i^{\alpha0}$ of the local minimum can be obtained as follows: When expanding the total potential energy around a set of $r_i^{\alpha0}$'s ($i=1,2,\ldots,3N$; $\alpha=x$, y, or z):

$$V[r_i^{\alpha0}+\sigma_i^\alpha]\approx V[r_i^{\alpha0}]-\sum_{i,\alpha}\sigma_i^\alpha F_i^\alpha[r_j^{\beta0}]+\sum_{i\alpha,j\beta}\sigma_i^\alpha\sigma_j^\beta H_{i,j}^{\alpha,\beta}[r_k^{\gamma0}]/2\ , \tag{1}$$

a set of the position coordinates of the local minimum are such that

$$F_i[r_j^{\alpha0}]=0\ , \tag{2}$$

and, at the same time, the eigenvalues of the Hessian $H_{i,j}^{\alpha,\beta}[r_k^{\gamma0}]$ satisfy

$$\omega_s[r_i^{\alpha0}]>0 \text{ for any } s\ (s=1,2,\ldots,3N-3)\ . \tag{3}$$

In Eq. (3) three vanishing eigenvalues, corresponding to the parallel motion of all particles, are excluded.

For the sake of simplicity, we shall adapt the following procedure to obtain the position coordinates of local minima: Position coordinates are calculated so that $|F_i^\alpha[r_j^\beta(t)]|<0.1$, and $\omega_s[r_i^\alpha(t)]>0$ for any s ($s=1,2,\ldots,3N-3$). Here, a set of $r_i^\alpha(t)$ is the time-dependent position coordinate, obtained by very promptly quenching the system from the present temperature to a very low temperature, say 10^{-3} K. By use of this procedure, we can obtain the exact position coordinates within an error of several percents.

III. HAMILTONIAN DYNAMICS AND GLASS

A. Four types of dynamics

We here study the system of 108 particles. The potential surface spans a 324- ($=3\times108$) dimensional space. To study the dynamics, five samples were prepared by cooling the system from a high to a low temperature. Five samples are assigned as 1–5. Differences between samples are produced by changing the time intervals during which the system runs at high temperatures, keeping the total energy fixed. The dynamics at each temperature

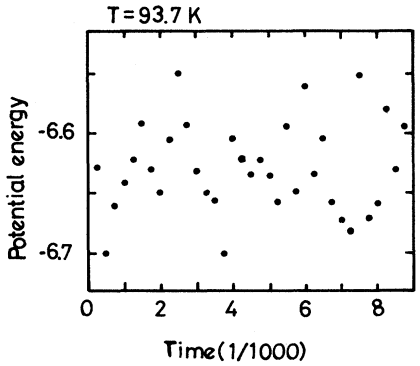

FIG. 1. The typical behavior of local minima on which the state point wanders in the high-temperature regime, which is that of sample 1, where temperature $T=93.7$ K. Units of potential energy and time are 167×10^{-16} erg and 2×10^{-14} sec.

is traced by keeping the total energy fixed; so kinetic energy or temperature is allowed to change. We shall study the Hamiltonian dynamics for the system left after it is cooled rapidly enough to bypass crystallization.

Four types of dynamics are found, depending on the temperatures. Hereafter, the regimes where they appear will be called high temperature, intermediate temperature, low intermediate temperature, and low temperature. The temperatures distinguishing them from each other are denoted as T_1, T_2, and T_3. In the following, T is assumed to be lower than the boiling temperature.

(1) The high-temperature regime: $T_1 \leq T$. Typical behavior of the local minima is indicated in Fig. 1. The local minima are monitored every 250 time steps. The local minima are widely distributed and as time elapses, the state point wanders over the various local minima. There is no tendency for the state point to stop wandering over the various local minima. The system is in a liquid state at this temperature.

(2) The intermediate-temperature regime: $T_2 \leq T < T_1$. The typical behavior of the local minima is shown in Fig. 2. The state point wanders over the energetically widely spread local minima for a specific time interval after system cooling stops. The behavior of the local minima is analogous to that in the liquid state. As time elapses, the state point gradually tends to stay in a single local minimum or a few local minima with almost equal potential energy. In the final state, the system shows only a small diffusion because it can only move over a few local minima. Then, the system is considered to be in a solid state. Thus, it is the relaxation of the system from the supercooled liquid to the solid. Here, the solid corresponds to a crystalline state, as will be shown later. The values of the potential energies at the local minima, in which the state point finally stays, depend on the samples. This means that there are many crystalline states.

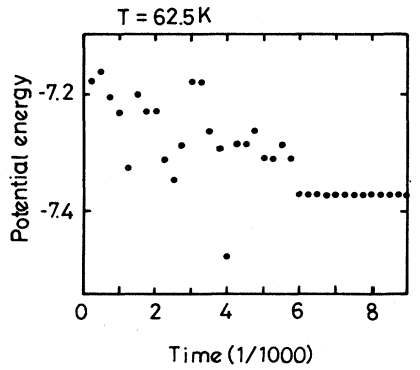

FIG. 2. The typical behavior of local minima on which the state point wanders in the intermediate-temperature regime, which is that of sample 1, where temperature $T=62.5$ K. Units of potential energy and time are 167×10^{-16} erg and 2×10^{-14} sec.

(3) The low–intermediate-temperature regime: $T_3 \leq T < T_2$. The dynamics of this regime differs on two points from that of the intermediate-temperature regime. Fluctuation of potential energies at the local minima for the certain time interval after system cooling stops is strongly suppressed and crystallization occurs through sequential phase locking, i.e., moving on several local minima sequentially. The typical behavior of the local minima is shown in Fig. 3. The state point stays in a single or the few local minima with almost equal potential energy for a specific time interval after system cooling stops. After that, the state point assumes the several lo-

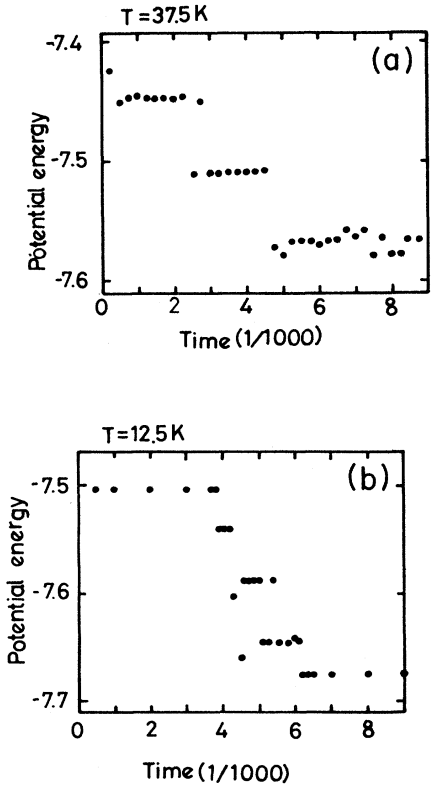

FIG. 3. The typical behavior of local minima on which the state point wanders in the low–intermediate-temperature regime. The behaviors of local minima in (a) and (b) correspond to those of sample 1 where temperature $T=37.5$ and 12.5 K, respectively. Units of potential energy and time are 167×10^{-16} erg and 2×10^{-14} sec.

TABLE I. Sample dependence of three characteristic temperatures T_1, T_2, and T_3. The temperature unit is 125 K.

Sample no.	1	2	3	4	5
T_1	0.55	0.55	0.55	0.50	0.50
T_2	0.30	0.40	0.35	0.40	0.40
T_3	0.05	0.05	0.05	0.05	0.15

cal minima intermittently and finally relaxs into a single local minimum or a few local minima with almost equal potential energy. As will be shown later, the final state is a crystalline state. The state point stays in a single local minimum or a few local minima at each stage of the stepwise crystallization. The appearances of local minima at each stage of the stepwise crystallization correlate with each other because crystallization proceeds only for a short time. As temperature decreases, the time interval for which the state point stays in a single or a few local minima with almost equal potential energy after system cooling stops becomes longer. As temperature decreases further, the state point enters the final temperature regime, i.e., the low-temperature regime.

(4) The low-temperature regime: $T < T_3$. The typical behavior of the local minima is shown in Fig. 4. The state point stays in a singlet local minimum or a few local minima with almost equal potential energy for the entire time interval. The number of local minima is quite small and so the diffusion becomes negligibly small. Any macroscopic diffusion is absent. The system is considered to be in a solid or glassy state. However, the relaxation for the structure can occur when the state point wanders over a few local minima, while it is arrested when the state point stays in a single local minimum.

The temperatures T_1, T_2, and T_3 depend on the samples, listed in Table I.

B. Packing structure and distance between two adjacent local minima at each temperature regime

In the following, structure of the system at its local minimum is called "inherent structure," following Stillinger and Weber.[19] The pair-correlation functions at local minima for high-temperature and low-temperature regimes are shown in Fig. 5. The pair-correlation functions monitored for a specific time interval after system cooling stops at the intermediate-temperature and the low–intermediate-temperature regimes are also shown in Fig. 6. From these figures, the packing structures are very similar or identical to each other. As has been noted,[19] the characteristic subpeak splitting of the second peak of the pair-correlation function occurs even in the packing structure at the local minima at the high-temperature regime. This suggests that the inherent structure of the liquid is frozen merely at a low temperature. The inherent structure of the liquid is close to random packing of the hard sphere, i.e., a homogeneous ran-

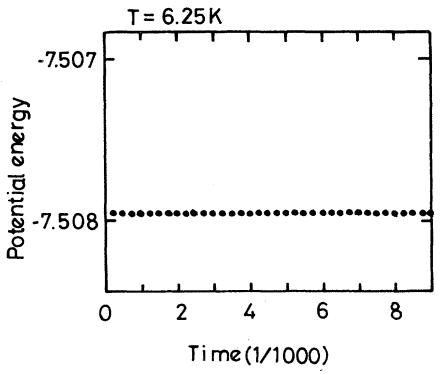

FIG. 4. The typical behavior of local minima on which the state point wanders in the low-temperature regime, which is that of sample 1, where temperature $T=6.25$ K. Units of potential energy and time are 167×10^{-16} erg and 2×10^{-14} sec.

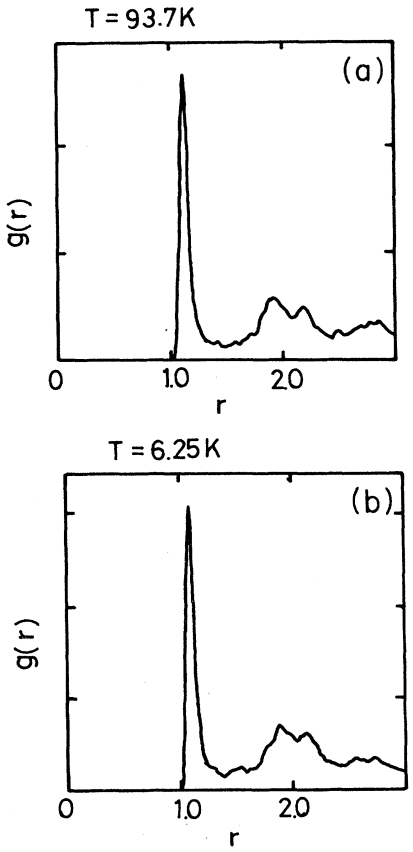

FIG. 5. The pair-correlation functions $g(r)$ of local minima in the high-temperature and low-temperature regimes. The pair-correlation functions in (a) and (b) correspond to those of sample 1 where $T=93.7$ and 6.25 K, respectively. The radial distance unit is 3.40 Å.

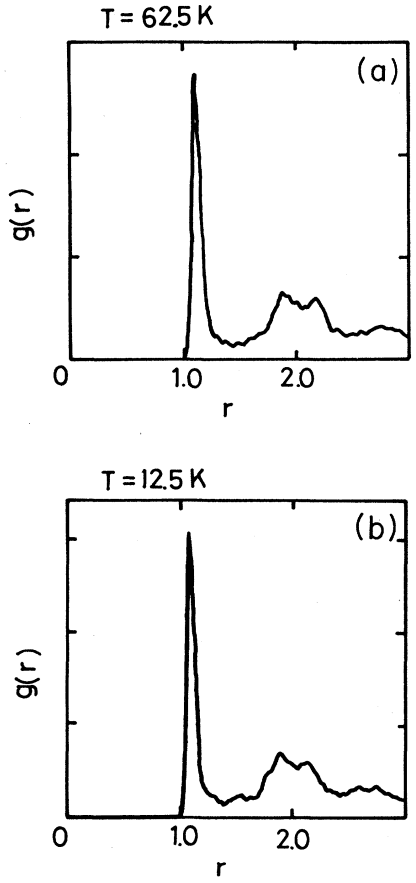

FIG. 6. The pair-correlation functions $g(r)$ of the local minima in the intermediate-temperature and low–intermediate-temperature regimes when the state point starts to run after the system cooling stops. The system is in the liquid state. The pair-correlation functions in (a) and (b) correspond to those of sample 1 where $T=62.5$ and 12.5 K, respectively. The radial distance unit is 3.40 Å.

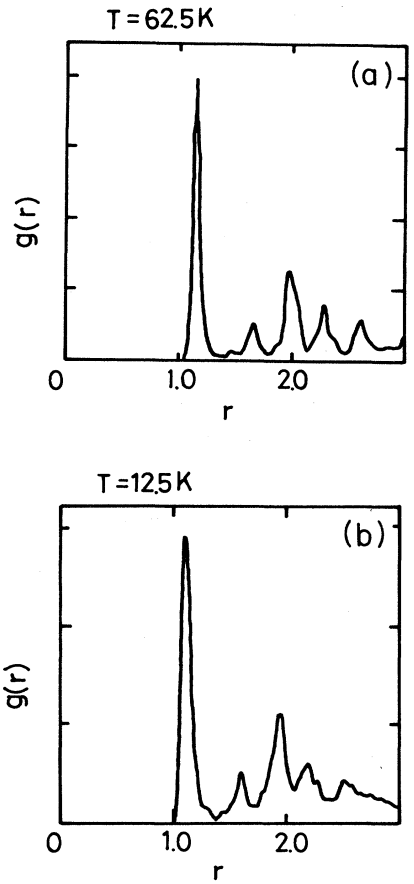

FIG. 7. The pair-correlation functions $g(r)$ of the local minima in the intermediate-temperature and low–intermediate-temperature regimes when the state point runs for a long time after the system cooling stops. The system is in the crystalline state. The pair-correlation functions in (a) and (b) correspond to those of sample 1 where $T=62.5$ and 12.5 K, respectively. The radial distance unit is 3.40 Å.

dom packing structure.

On the other hand, after the state point runs for a long time, it stays in a single or a few local minima in the intermediate-temperature and low-temperature regimes. The pair-correlation functions of the packing structure are shown in Fig. 7. It is not difficult to examine these packing structures. The pair-correlation functions are similar to that of the hexagonal-closed-packed (hcp) and the face-centered-cubic (fcc) packing structures, as indicated in Fig. 8. The second peak splitting of the pair-correlation function that appeared in the random packing disappears here. In particular, the second ($\simeq 1.6$) and third ($\simeq 1.9$) peaks indicate the growth of a layer of hexagonal close packing. The existence of satellite peaks near the third and the fourth peaks in Fig. 7 indicate that the packing structure is very similar to the mixture of the hcp and the fcc packing structures, i.e., the random stacking of layers of hexagonal close packing. This is a reasonable mixture from the fact that the potential-energy difference among the hcp, the fcc, and the random-hexagonal-close-packing structures is less than 1%. The packing structure has been previously examined, and found[20] to be a stacking of layers with stacking faults, where each layer forms a close packed structure with occasional defects.

Next we examine the distance between two adjacent local minima over which the state point wanders. The distance is defined by

$$d^{i,j}=\left[\sum_{k,\alpha}|r_k^{\alpha i}-r_k^{\alpha j}|^2\right]^{1/2}.$$

Here, a set of $r_k^{\alpha i}$ and $r_k^{\alpha j}$ are the position coordinates coordinates for two adjacent local minima denoted by i and j. The distances $d^{i,j}$ are shown in Fig. 9 as a function of potential-energy difference $\Delta E_{i,j}$ between two adjacent local minima over which the state point wanders at the high-temperature regime. The distances are monitored at every other time step. The distribution of distances is scattered, and all distances are not small. That the maximum value of

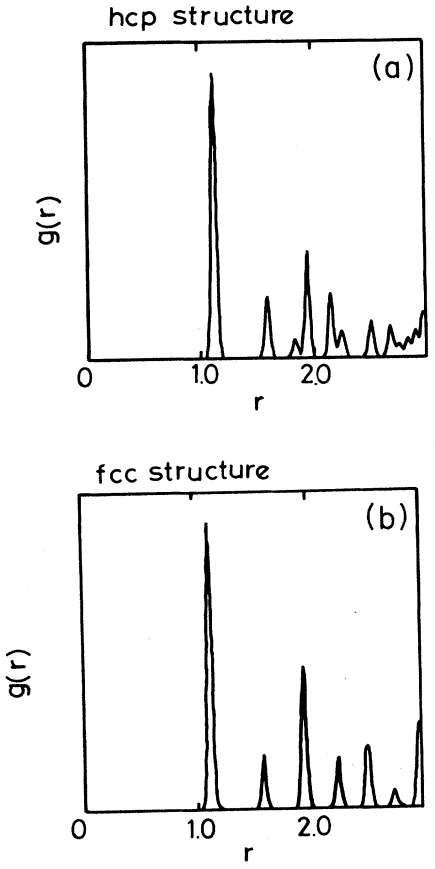

FIG. 8. The pair-correlation functions $g(r)$ of (a) hexagonal-close-packing and (b) face-centered-cubic-packing structures. Although the peaks in the pair-correlation functions have the Dirac measure, they are slightly broadened for the sake of comparing the pair-correlation functions of the hcp and fcc structures with those in Figs. 7(a) and 7(b). The radial distance unit is 3.40 Å.

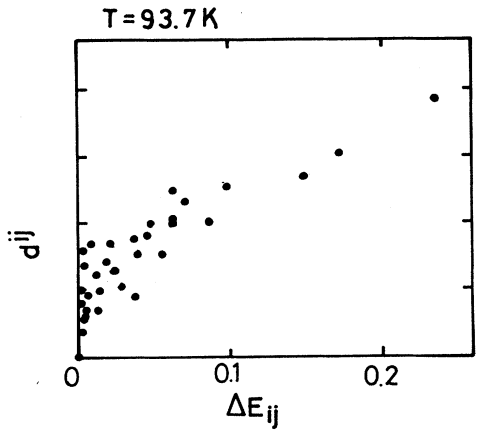

FIG. 9. The distances $d^{i,j}$ as a function of the difference $\Delta E_{i,j}$ of the potential energies of two adjacent local minima denoted by i and j on which the state point wanders every other step for sample 1 where $T=93.7$ K. The distances normalized by the number of particles, i.e., $d^{i,j}/\sqrt{N}$ ($N=108$) are given in the figure. All distances are not small. The general rule for transition between local minima is that a large (or small) distance between the local minima corresponds to a large (or small) difference of the potential energies at the local minima. Units of potential energy and length are 167×10^{-16} erg and 3.40 Å.

$$\left[\sum_{\alpha}|r_k^{\alpha i}-r_k^{\alpha j}|^2\right]^{1/2}$$

($k=1,2,\ldots,N$) is not different from the average value $d^{i,j}/\sqrt{N}$ of the distance shows that only a few k's of

$$\left[\sum_{\alpha}|r_k^{\alpha i}-r_k^{\alpha j}|^2\right]^{1/2}$$

do not contribute to $d^{i,j}$, that is, the configurational change between two adjacent local minima is not localized. This property is in contrast to that found in the low-temperature regime, as will be seen later. However, the distance is less than $\sqrt{N}$. This implies that the region over which transition occurs is larger than the atomic size but less than the system size. This property holds for the liquid state and also when the state point wanders intermittently between local minima during crystallization at $T_3\leq T<T_2$. It also holds for the liquid state when the system begins to run in the intermediate-temperature regime. The distances for the crystallization process are also listed in Table II for sample 1. As seen from Fig. 9, the general rule for transition is that a large (or small) distance between the local minima corresponds to a large (or small) difference between the potential energies at the two adjacent local minima. This also holds for the other transitions occurring during crystallization and in the solid state.

The distances between two adjacent local minima for the system after crystallization occurs, for the system beginning to run in the low–intermediate-temperature regime, and for the solid state at the low temperature, is in sharp contrast to those of the previous case. From studies of the distances between two adjacent local minima and the distribution of

$$\left(\sum_{\alpha}|r_k^{\alpha i}-r_k^{\alpha j}|^2\right)^{1/2},$$

it is found that the configurational change occurs only over a few particles, i.e., the transition is localized and so the distance between two adjacent local minima is very small. This result completely agrees with the picture of the glassy state of Goldstein.[14]

C. Glass and glass transition

At which temperature is a glassy solid formed and where does glass transition occur? As seen in the previous subsection, the packing structure of the glassy solid is similar to that of the inherent structure of the local minima, which does not assume crystallization. Imagine that we observe the system for a certain time interval to monitor physical quantities after the system is cooled to an arbitrary temperature. Then, at $T<T_2$, the system

TABLE II. Top: Distances $d^{i,j}$ between adjacent local minima for two transitions in Fig. 3(a). Potential energies of local minima are denoted by E_1, E_2, and E_3. The distances normalized by the number of particles, i.e., $d^{i,j}/\sqrt{N}$ ($N=108$) are given in the table. Units of potential energy and length are 600 K and 3.4 Å. Bottom: Distances $d^{i,j}$ between adjacent local minima for four transitions in Fig. 3(b). Potential energies of local minima are denoted by E_1, E_2, E_3, E_4, and E_5. The distances normalized by the number of particles, i.e., $d^{i,j}/\sqrt{N}$ ($N=108$) are given in the table. Units of potential energy and length are 600 K and 3.4 Å.

Potential energy	$E_1=-7.448$	$E_2=-7.508$	$E_3=-7.676$		
Distance $d^{i,j}$	$d^{1,2}=0.336$	$d^{2,3}=0.271$			
Potential energy	$E_1=-7.503$	$E_2=-7.540$	$E_3=-7.587$	$E_4=-7.646$	$E_5=-7.676$
Distance $d^{i,j}$	$d^{1,2}=0.236$	$d^{2,3}=0.247$	$d^{3,4}=0.175$	$d^{4,5}=0.306$	

wanders only over a few local minima with almost equal potential energy for a specific time interval after system cooling stops, that is, the system behaves as a solid because of its small diffusion. At $T_2 \leq T$, the system behaves as a liquid after system cooling stops. Here, we can specify the "specific" time interval by the time interval until crystallization occurs. Furthermore, the number of local minima can be measured by entropy. The entropy relates to the specific heat such that the decrease in the number of the local minima produces the drop in the heat capacity for $T < T_2$. Thus, it might be concluded that T_2 corresponds to the glass transition, and the glassy solid is formed at $T < T_2$. The value of T_2 depends on samples: $T_2 = 37-60$ K, which almost agrees with the glass transition temperatures previously concluded.[4,8,11,12] However, it should be emphasized that the arguments used to determine the glass transition temperature quite differ from those of the others. Discussions analogous to ours have been given by emphasizing the growth of the icosahedral ordering of particles.[21]

As has often been done,[8,10,12] the analogous behavior of the specific heat can be derived from the appearance of a break in the enthalpy versus temperature curve. However, the method seems suspicious to me. The volume of the system changes with decreasing temperature. This change results in the break in the enthalpy versus temperature. For example, when enthalpies are calculated as a function of temperature for two systems with the same volume, the system obtained to bypass crystallization and that of the fcc packing structure, the break appears in the fcc packing structure although no change occurs in the dynamical property.

IV. DISCUSSION

So far, we have examined Hamiltonian dynamics to study the formation process of a glassy solid. We found four types of dynamics, depending on the temperature, which are classified by three characteristic temperatures: T_1, T_2, and T_3. A glassy solid is formed for $T < T_2$, and a glass transition temperature is assigned to T_2.

Finally, we shall discuss the landscape of the potential surface over which the state point wanders and its dependence on the type of the interaction potential. In the low-temperature regime, the state point stays at a single local minimum or a few local minima. The picture of how the state point moves on the potential surface is as follows. A potential barrier is formed in an arbitrary direction around the local minimum point. The potential barrier is high in certain directions and low towards others. This barrier has various heights depending on the direction from the local minimum point. In the low-temperature regime, the state point follows the direction of the lowest potential barrier. That is, the direction in which the state point moves is very limited due to the small kinetic energy. Generally, the potential barrier is expected to be lower as the distance between two adjacent local minima decreases. Then, the transition between two adjacent local minima occurs between local minima within a short time. The transition is adequately described by using a reaction coordinate. Next suppose that the temperature or kinetic energy increases. Then the transition of the state point can go across the higher potential barrier, or, is also not allowed to go along the reaction coordinate between the local minima. This picture is especially valid for the liquid state in the high-temperature and intermediate-temperature regimes. The transition is generally not localized. As seen from Fig. 9, this transition occurs frequently. This fact has been noted[14] as failure of the potential-barrier description of the viscous flow when temperature arises.

Why is the transition at the low–intermediate-temperature regime so sharp? Why does the LJ system have a strong tendency to crystallization, that is, why is the potential barrier so low towards crystallization? Let us examine the diffusion of each particle when crystallization is just occurring. In Fig. 10, the diffusion length of each particle is shown as a function of time for a transition occurring at $t \simeq 4400$ in Fig. 3(b). Particles 11 and 69 diffuse very quickly in the early stage of transition. After they cease diffusion, the other particles begin to diffuse. This implies that particles 11 and 69 work as a trigger for the diffusion of the other particles. The trigger particles responsible for the crystallization are small, and so the potential barrier to crystallization is small. The same thing is found for the other transitions in sample 1 and for transitions of the other samples, although the number of trigger particles is not necessarily two. Cascade diffusion of the other particles following the motion of the trigger particles increases the distance between two adjacent local minima by which the state point transmits. That the transition is sharp is understood from the fact that only a few particles work as a trigger for the crystallization. The reason why crystallization occurs by assuming several local minima sequentially cannot be understood by the conventional picture[22,23] in which crystallization occurs through two

steps. (i) First the crystallization centers, i.e., the nuclei occasionally appear through the nucleation by thermal fluctuation and (ii) it then grows by lowering the free energy. At a high temperature, (i) proceeds well but (ii) is suppressed, while, at a low temperature, (i) is suppressed by small thermal fluctuations but (ii) proceeds well. It seems more appropriate to consider that crystallization occurs by sequentially dissolving defects that pin the amorphous packing.

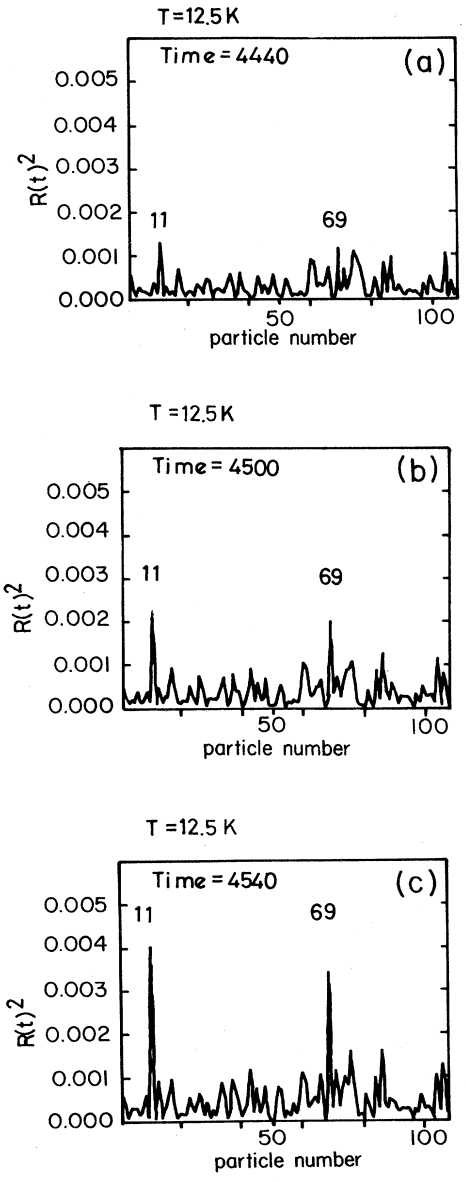

FIG. 10. The diffusion length $R_i(t)$ of each particle as a function of particle number for the transition occurring near $t=4400$ in Fig. 3(b). (a), (b), and (c) corresponds to $t=4400$, 4500, and 4540, respectively. $R_i(t)^2$ is defined by $R_i(t)^2=\sum_\alpha |r_i^\alpha(t)-r_i^\alpha(s)|^2$, where s is taken to be $s=4400$. Units of length and time are 3.40 Å and 2×10^{-14} sec. It should be noted that the $R(t)^2$ given in the figure is the square of the diffusion length $R_i(t)$.

Different from the case of systems that interact with a two-body potential such as the LJ and the Morse potentials, the materials with covalent bonding, such as SiO_2 and polymers have a strong anisotropy for their interaction potential. We can easily imagine then, that the potential surface also has a strong anisotropy, even for a small region on the potential surface, due to the anisotropic interaction. Then, the potential barrier is low in a certain direction on the potential surface, but is much higher in any other direction. As a result, diffusion decreases, i.e., the system becomes vitreous. For this reason, these systems are considered to have a strong tendency towards glass forming.

Consider the systems interacting with a two-body potential such as the LJ and the Morse potentials. The difference between them may then appear in the strength of the nonlinearity of the interaction potential. For example, let us consider the simplest case of a harmonic potential where the total potential energy is precisely expanded into a quadratic form over the entire potential surface. Then, a single local minimum is only formed on the potential surface since the total potential energy is expressed by Eq. (1) over the entire region of particle position coordinates. This example suggests that the number of the local minima increases as the interaction potential has the stronger nonlinearity, that is, higher-order terms than the quadratic terms, when the interaction potential is expanded in terms of the small-particle displacements around the local minimum, become more appreciable. The number of the local minima has been studied for a microcluster, which consists of 13 particles.[24] The number of the local minima is *much* less for the Morse potential than for the LJ potential: the number of the local minima is 988 for the LJ potential system and 36 for the Morse potential system. The question of whether the LJ or the Morse potential has stronger nonlinearity might be answered, for example, by examining the change of the second derivatives of the potential with respect to the distance between particles when the distance between particles varies around a distance corresponding to the potential minimum. This study implies that density of the local minima is much higher for the LJ systems than for the Morse potential systems. It is expected that the low (or high) density of the local minima yield a high (or low) potential barrier between local minima. The Morse potential system is considered to have a stronger tendency towards the glass forming that the LJ system. This agrees with the observation that monatomic Al forms glass by using laser quenching,[25] although the LJ system has never formed glass, since the interaction potential of metallic substances is well described by the Morse potential.

ACKNOWLEDGMENTS

The author wishes to thank Dr. K. Otuka for his useful discussions and encouragement, and Professor T. Sasada for his critical support.

[1]*Glassy Metals (I),* edited by H.-J. Güntherodt and H. Beck (Springer-Verlag, Berlin, 1981); *Glassy Metals (II),* edited by H. Beck and H.-J. Güntherodt (Springer-Verlag, Berlin, 1983).

[2]*Science and Technology,* edited by D. R. Uhlmann and N. J. Kreidl (Academic, New York, 1983), Vol. 1; *Science and Technology,* edited by D. R. Uhlmann and N. J. Kreidl (Academic, New York, 1985), Vol. 3.

[3]L. V. Woodcock, C. A. Angell, and P. Cheeseman, J. Chem. Phys. **65**, 1565 (1976).

[4]A. Rahman, M. J. Mandell, and J. P. Mctague, J. Chem. Phys. **65**, 1564 (1976).

[5]W. D. Kristensen, J. Non-Cryst. Solids **21**, 303 (1976).

[6]M. J. Mandell, J. P. Mctague, and A. Rahman, J. Chem. Phys. **66**, 3070 (1977).

[7]H. R. Wendt and F. F. Abraham, Phys. Rev. Lett. **41**, 1244 (1978).

[8]J. H. R. Clarke, J. Chem. Soc. Faraday Trans. II **75**, 1371 (1979).

[9]F. F. Abraham, J. Chem. Phys. **72**, 359 (1980).

[10]C. A. Angell, J. H. R. Clarke, and L. V. Woodcock, Adv. Chem. Phys. **48**, 397 (1981) (herein, many references of molecular-dynamics studies for simple liquids).

[11]M. Kimura and F. Yonezawa, in *Topological Disorder in Condensed Matter,* edited by F. Yonezawa and T. Ninomiya (Springer-Verlag, Berlin, 1983), p. 80.

[12]J. R. Fox, and H. C. Andersen, J. Chem. Phys. **88**, 4017 (1984).

[13]K. Shinjo, J. Chem. Phys. **90**, 6627 (1989).

[14]M. Goldstein, J. Chem. Phys. **51**, 3728 (1969).

[15]F. H. Stillinger and T. A. Weber, Science **225**, 983 (1984).

[16]F. H. Stillinger and T. A. Weber, Phys. Rev. A **28**, 2408 (1983).

[17]The Lennard-Jones system can form glasslike solids only with very rapid cooling rates, say 10^{12} K/sec. This is considered too rapid to be achieved under laboratory conditions. However, a laser quenching technique may be useful in accomplishing this very rapid cooling rate (see Ref. 25).

[18]For example, see, *Molecular-Dynamics Simulation of Statistical Systems,* Proceedings of the International School of Physics "Enrico Fermi" Course XC, edited by G. Ciccotti and W. G. Hoover (North-Holland Physics, Italy, 1986).

[19]F. H. Stillinger and T. A. Weber, J. Chem. Phys. **80**, 4434 (1984).

[20]S. Nosé and F. Yonezawa, J. Chem. Phys. **84**, 1803 (1985).

[21]H. Jónsson and H. C. Andersen, Phys. Rev. Lett. **60**, 2295 (1988).

[22]W. Kauzmann, Chem. Rev. **43**, 219 (1943).

[23]D. Turnbull, Contemp. Phys. **10**, 473 (1969).

[24]M. Hoare, Adv. Chem. Phys. **40**, 47 (1979).

[25]M. von Allman, *Glassy Metals (II)* (Springer-Verlag, Berlin, 1983), p. 261.